J Appl Electrochem (2010) 40:163–173
DOI 10.1007/s10800-009-9992-1

ORIGINAL PAPER

Antibacterial drugs as inhibitors for the corrosion of stainless steel type 304 in HCl solution

A. S. Fouda · H. A. Mostafa · H. M. El-Abbasy

Received: 9 March 2009 / Accepted: 16 August 2009 / Published online: 2 September 2009
© Springer Science+Business Media B.V. 2009

Abstract The effect of three antibacterial drugs (3-thiazinonyl-bicyclo [4.2.0] octene-carboxylate derivatives) on the corrosion behavior of stainless steel type 304 in 1.0 M HCl solution has been investigated using weight loss, potentiodynamic polarization, and electrochemical impedance spectroscopy (EIS) techniques. The inhibition efficiency increased with increase in inhibitor concentration but decreased with increase in temperature. The thermodynamic functions of corrosion and adsorption processes were evaluated. The potentiodynamic polarization measurements indicated that the inhibitors are of mixed type. The adsorption of these inhibitors was found to obey Langmuir's adsorption isotherm. Synergism between iodide ion and inhibitors was proposed. The inhibitive action was satisfactory explained by using both thermodynamic and kinetic models. The results obtained from the three different techniques were in good agreement.

Keywords Corrosion · HCl · Antibacterial drugs · Stainless steel type 304

1 Introduction

Stainless steel type 304 has found wide applications in variety of industries. It is covered with a highly protective film of chromium ox-hydroxide and is resistant to corrosion in many aggressive environments. It is possible to reduce the corrosion rate to safe level by adding inhibitors. Organic compounds and their derivatives were used successfully as inhibitors for different types of steels and were studied extensively through the last century. Recently, interest is still growing for exploiting other inhibitors for the corrosion of stainless steels [1]. Several organic molecules containing sulfur, oxygen, and nitrogen hetero-atoms were suggested as inhibitors for steel in acidic medium [2–8]. A few investigators have been reported on the use of antibacterial drugs as corrosion inhibitors [9–13]. Sulpha drugs have been reported also as corrosion inhibitors by several authors [14–16]. Schiff bases that are derived from sulpha drugs and many of their complexes exhibit a wide range of corrosion inhibition effects [17–20].The inhibition mechanism for this class of inhibitors is mainly based on adsorption [21]. The present investigation aimed to study the effect of three 3-thiazinonyl-bicyclo[4.2.0] octene-carboxylate derivatives as inhibitors for the corrosion of stainless steel type 304 in 1.0 M HCl. Also, the relationship between calculated quantum chemical parameters and experimental inhibition efficiencies of the inhibitors was discussed.

2 Experimental methods

2.1 Materials

The experiments were performed with stainless steel type 304 specimens in the form of rods and sheets with the following composition: $C = 0.1\%$, Mn $= 0.5\%$, $P = 0.025\%$, $S = 0.025\%$, Fe remainder.

2.2 Solutions

The aggressive solutions used were made of AR grade HCl. Appropriate concentrations of acid were prepared using

A. S. Fouda (✉) · H. A. Mostafa · H. M. El-Abbasy
Department of Chemistry, Faculty of Science, El-Mansoura University, El-Mansoura 35516, Egypt
e-mail: asfouda@mans.edu.eg

distilled water. From the investigated compounds, 10^{-3} M stock solutions were prepared by dissolving the appropriate weights of the used chemically pure solid compounds in distilled water.

2.3 Weight loss method

Three parallel stainless steel sheets of 2 × 2 × 0.2 cm were abraded with emery paper up to 1200 grit and then washed with distilled water and acetone. After weighing accurately, the specimens were immersed in 100 ml beaker, which contained 100 ml HCl with and without addition of different concentrations of inhibitors. All the aggressive acid solutions were open to air. After 6 h, the specimens were taken out, washed, dried, and weighed accurately. The average weight loss of the three parallel stainless steel sheets could be obtained. Then the tests were carried out at a temperature range 25–55 °C. The inhibition efficiency (IE) and the degree of surface coverage (θ) at different concentrations (1×10^{-6} to 5×10^{-4} M) of investigated inhibitors on the corrosion of stainless steel were calculated as follows [22]:

$$\mathrm{IE}\% = [(W_o - W)/W_o] \times 100 \quad (1)$$

$$\theta = [(W_o - W)/W_o], \quad (2)$$

where W_o and W are the values of the average weight loss without and with addition of the inhibitor, respectively.

2.4 Potentiodynamic polarization measurements

Polarization experiments were carried out in a conventional three-electrode cell with a platinum counter electrode and a saturated calomel electrode coupled to a fine Luggin capillary as the reference electrode. The working electrode was in the form of a square cut from stainless steel sheet (1 cm × 1 cm) embedded in epoxy resin of polytetrafluoroethelene so that the flat surface was the only surface in the electrode. Before polarization scanning, working electrode was immersed in the test electrolyte of 100 ml in volume for 20 min until steady state, and the open circuit potential (OCP) was attained which was taken as E_{OC}. All potentiodynamic measurements were carried out with a Gamry framework instruments (version 3.20), controlled by a computer which also recorded and stored the data. All experiments were carried out at 25 ± 1 °C using Lab companion circulator thermostat model CW-05GL, and solutions were not dearated. For polarization measurements potential from −300 to 100 mV (relative to open circuit potential, E_{OCP}) was applied, while potential from −500 to 700 mV (relative to reference electrode potential, E_{ref}) was applied in case of pitting measurements. IE% and the degree of surface coverage (θ) were defined as:

$$\mathrm{IE}\% = [(i_{corr} - i_{corr(inh)})/i_{corr}] \times 100 \quad (3)$$

$$\theta = \left[\left(i_{corr} - i_{corr(inh)}\right)/i_{corr}\right], \quad (4)$$

where i_{corr} and $i_{corr(inh)}$ are the uninhibited and inhibited corrosion current density values, respectively, determined by extrapolation of Tafel lines to the corrosion potential.

2.5 Electrochemical impedance spectroscopy method

The EIS spectra were recorded at OCP after immersion of the electrode for 10 min in the test solution. The AC signal was 5 mV peak to peak and the frequency range studied was between 100 kHz and 0.2 Hz. All electrochemical impedance experiments were carried out using Potentiostat/Galvanostat/Zra analyzer (Gamry PCI300/4). A personal computer with EIS 300 software and Echem Analyst 5.21 was used for data fitting and calculating.

The IE% and the surface coverage (θ) of the used inhibitors obtained from the impedance measurements can be calculated by applying the following relations:

$$\mathrm{IE}\% = [1 - (R_{ct}^{o}/R_{ct})] \times 100, \quad (5)$$

$$\theta = \left[1 - \left(R_{ct}^{o}/R_{ct}\right)\right], \quad (6)$$

where $R_{ct}^{o}$and R_{ct} are the charge transfer resistance in the absence and presence of inhibitor, respectively.

2.6 Inhibitors

The following three antibacterial drugs (3-thiazinonyl-bicyclo[4.2.0] octene-carboxylate derivatives) were used as inhibitors for the corrosion of stainless steel type 304 in 1 M HCl. The choice of these drugs as corrosion inhibitors is based on: (i) they can be easily produced and purified, (ii) they are healthy reportedly very important in biological reactions (environmentally friendly), (iii) easily soluble in water, and (iv) the molecules have O, N, and S atoms as active centers. Stock solutions (10^{-3} M) of Compounds [A–C] were prepared by dissolving the appropriate weight of each drug separately in double distilled water in 100 ml measuring flask.

A. (6R,7R,Z)-7-(2-(2-aminothiazol-4-yl)-2-(methoxyimino) acetamido)-3-(1-methyl pyrrolidinium-1-yl)methyl)-8-oxo-5-thia-1-aza-bicyclo[4.2.0]oct-2-ene-2-carboxylate

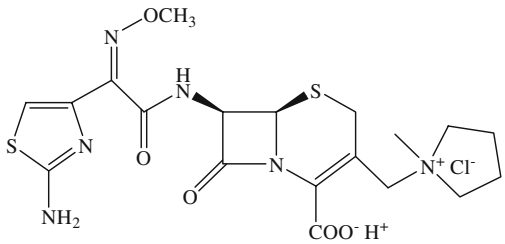

(Produced by Bristol-Myers Squibb Egypt Company, Egypt)
Chemical Formula: $C_{19}H_{25}ClN_6O_5S_2$, Molecular Weight: 517.02

B. (6R,7R,Z)-7-(2-(2-aminothiazol-4-yl)-2-(2-carboxypropan-2-yloxyimino) acetamido)-8-oxo-3-(pyridinium-1-ylmethyl)-5-thia-1-aza-bicyclo[4.2.0]oct-2-ene-2-carboxylate

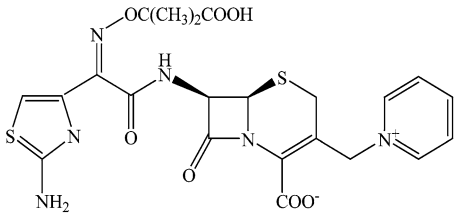

(Produced by Glaxo Smithkline Company, Egypt)
Chemical Formula: $C_{22}H_{22}N_6O_7S_2$, Molecular Weight: 546.58

C. (6R,7R,Z)-7-{[2-[(4-ethyl-2,3-dioxo-piperazine-1-carbonyl)amino]-2-(4-hydroxyphenyl)acetyl}amino]-3-[(1-methyltetrazol-5-yl)sulfanylmethyl]-8-oxo-5-thia-1-aza-bicyclo[4.2.0]oct-2-ene-2-carboxylic acid

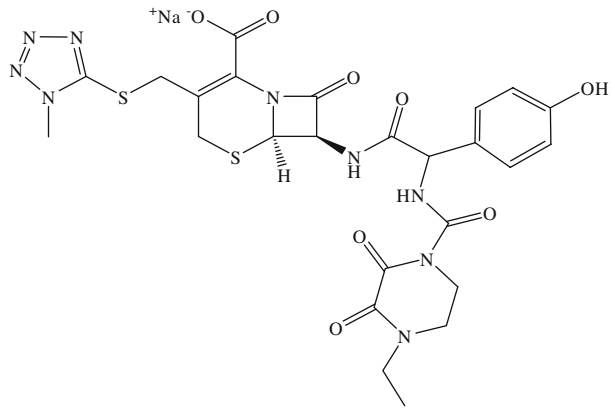

(Produced by Pharco Pharmaceutical Company, Egypt)
Chemical Formula: $C_{25}H_{26}N_9NaO_8S_2$, Molecular Weight: 667.65

3 Results and discussion

3.1 Weight loss measurements

The weight loss of stainless steel type 304 specimen in 1.0 M HCl solution, with and without different concentrations from the investigated inhibitors, was determined after 6 h of immersion at 25 °C. Figure 1 represents this for Compound (C) as an example. Similar curves were

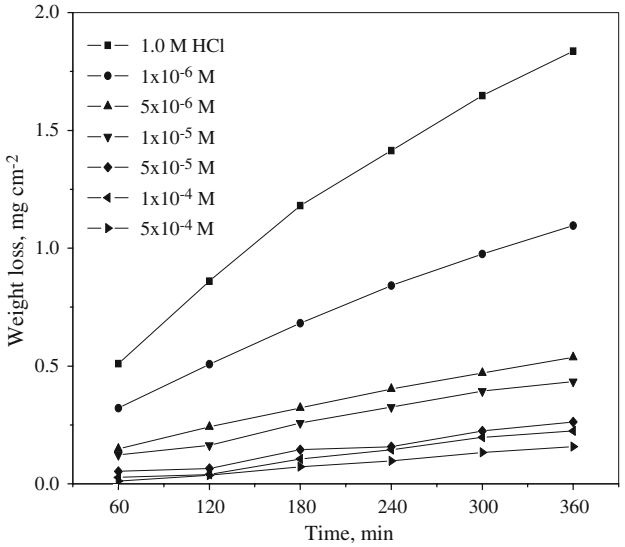

Fig. 1 Weight loss-time curves for the corrosion of stainless steel type 304 in 1.0 M HCl in the absence and presence of different concentrations of Compound (C) at 25 °C

obtained for other inhibitors (not shown). Obtained values of IE% are given in Table 1. The presence of inhibitors reduces the corrosion rate of steel in HCl.

3.1.1 Adsorption isotherm

One of the most convenient ways of expressing adsorption quantitatively is by deriving the adsorption isotherm that characterizes the metal/inhibitor/environment system [23]. Various adsorption isotherms were applied to fit θ values, but the best fit was found to obey Langmuir adsorption isotherm [24] which may be expressed by:

$$C/\theta = 1/\beta + C, \tag{7}$$

where C is inhibitor concentration and β is equilibrium constant of adsorption. It is well known that the standard adsorption free energy (ΔG^{o}_{ads}) is related to equilibrium constant of adsorption (β) and can be calculated by the following equation [25]:

$$\beta = (1/55.5)\exp\left[-\Delta G^{o}_{ads}/RT\right]. \tag{8}$$

Figure 2 represents the plot of (C/θ) against C for all investigated compounds. Also, it is found that the kinetic–thermodynamic model of El-Awady et al. [26], i.e.,

$$\log(\theta/1-\theta) = \log k' + y \log C \tag{9}$$

is valid to operate the present adsorption data. $\beta = \beta'^{(1/y)}$, β' is constant, and $1/y$ is the number of the surface active sites occupied by one inhibitor molecule and C is the bulk concentration of the inhibitor. Plotting $\log(\theta/1-\theta)$ against log C for the compounds is given in Fig. 3, where straight line relationships were obtained suggesting the validity of

Table 1 Binding constant (β), free energy of adsorption (ΔG^{o}_{ads}), and number of active sites ($1/y$) and for adsorption of Compounds (A), (B), and (C) and heat of adsorption (Q) of 5×10^{-5} M on stainless steel type 304 surface in 1.0 M HCl at 25 °C

Inhibitor	Kinetic model			Langmuir isotherm		$-Q$ (kJ mol^{-1})
	$1/y$	$\beta \times 10^{-5}$	$-\Delta G^{o}_{ads}$ (kJ mol^{-1})	$\beta \times 10^{-5}$	$-\Delta G^{o}_{ads}$ (kJ mol^{-1})	
A	2.1	2.1	40.3	1.8	39.9	15.0
B	2.6	6.0	42.9	3.5	41.6	16.7
C	2.1	9.2	44.0	4.1	42.0	23.6

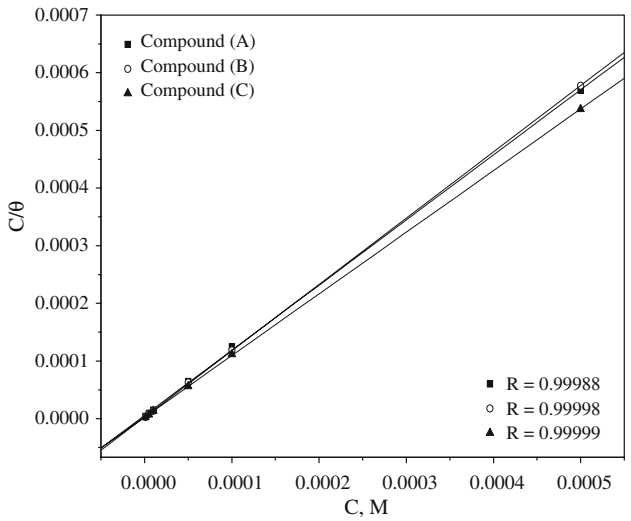

Fig. 2 Langmuir adsorption isotherm plotted as (C/θ) versus C of Compounds (A), (B), and (C) for corrosion of stainless steel type 304 in 1.0 M HCl solution at 25 °C

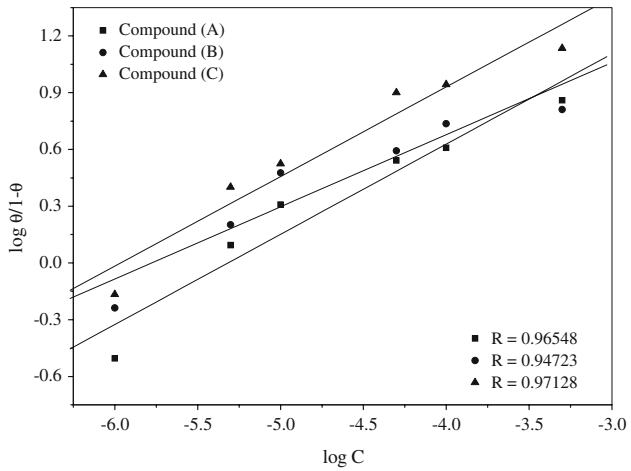

Fig. 3 El-Awady et al. [26] model plotted as $\log(\theta/1-\theta)$ versus $\log C$ of Compounds (A), (B), and (C) for corrosion of stainless steel type 304 in 1.0 M HCl solution at 25 °C

this model for the studied case. A plot of $\log(\theta/1-\theta)$ versus 1/T at constant additive concentrations (5×10^{-5} M) (Fig. 4) gives straight lines according to the following equation:

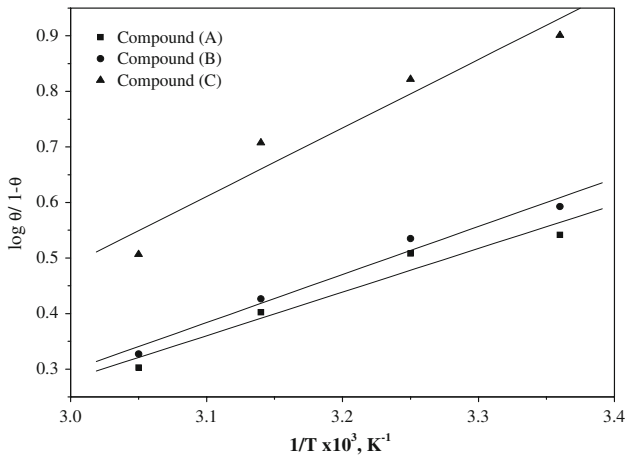

Fig. 4 Plots of $\log(\theta/1-\theta)$ versus $1/T$ for 5×10^{-5} M of Compounds (A), (B), and (C) for corrosion of stainless steel type 304 in 1.0 M HCl solution at 25 °C

$$\log \theta/1-\theta = \log A + \log C - (Q/2.303RT). \quad (10)$$

The Q values were obtained from the slopes of these lines. The values of β and ΔG^{o}_{ads} calculated by Langmuir isotherm and $1/y$, β, and ΔG^{o}_{ads} calculated by the kinetic model, and the values of Q are given in Table 1. The negative values of ΔG^{o}_{ads} suggest that the adsorption of inhibitor molecules onto steel surface is a spontaneous process. The magnitude of adsorption heat reaches the magnitude of chemical reaction heat, which is the result of the transference of electron from donating atoms in the inhibitor molecule to the *d*-orbital of the iron atom. The negative values of Q show that the process of adsorption is exothermal. It is noted that the value of $1/y$ is more than unity. This means that the given inhibitor molecules will form monolayer on the steel surface. In general, the values of ΔG^{o}_{ads} obtained from El-Awady et al. model are comparable with those obtained from Langmuir isotherms.

3.1.2 *Effect of temperature*

The effect of temperature on the rate of dissolution of stainless steel type 304 in 1.0 M HCl containing different concentrations of the investigated inhibitors was tested by

Table 2 Effect of temperature on the inhibition efficiencies of different concentrations of Compounds (A), (B), and (C) for the corrosion of stainless steel type 304 in 1.0 M HCl

Temp. T (°C)	Inhibitor	IE (%)					
		[Inhibitor] (M)					
		1×10^{-6}	5×10^{-6}	1×10^{-5}	5×10^{-5}	1×10^{-4}	5×10^{-4}
25 °C	A	23.8	55.4	67.0	77.7	80.3	87.9
	B	36.6	61.4	75.0	79.6	84.5	86.6
	C	40.5	75.5	77.0	88.8	89.8	93.2
35 °C	A	–	53.3	59.0	76.3	78.1	87.8
	B	–	56.6	70.5	77.4	79.3	86.9
	C	–	68.6	75.1	86.9	88.9	93.5
45 °C	A	–	35.2	51.8	71.6	73.5	85.4
	B	–	39.9	58.5	72.8	76.9	84.4
	C	–	51.2	64.2	83.6	86.3	90.8
55 °C	A	–	28.7	42.5	66.7	68.7	83.5
	B	–	33.0	46.7	68.0	72.9	82.6
	C	–	29.3	44.3	76.2	83.4	91.9

weight loss method over a temperature range from 25 to 55 °C. The effect of increasing temperature on the IE values is listed in Table 2. The results revealed that on increasing temperature there is an increase of weight loss while IE decreases for all compounds used.

The activation energy of the corrosion process was calculated using the Arrhenius equation [27]:

$$R_{\text{corr}} = A \exp\left(-E_{\text{a}}^{*}/RT\right), \tag{11}$$

where R_{corr} is the corrosion rate, A is the pre-exponential factor, E_{a}^{*} is the apparent activation energy, R is the universal gas constant, and T is the absolute temperature. The apparent activation energy at 5×10^{-5} M from the investigated compounds was calculated by linear regression between ln R_{corr} and $(1/T)$ (Fig. 5). The values of E_{a}^{*} can be obtained from the slope of the straight lines were found to be 44.3 kJ mol^{-1} in 1.0 M HCl and 55.2, 56.6, and 64.0 kJ mol^{-1} in the presence of Compounds (A), (B), and (C), respectively.

The activation energy is higher in the presence of additives than in their absence. Similar results were obtained by other authors [25, 28–30]. The higher values of E_{a}^{*} are good evidence for the strong adsorption of 3-thiazinonyl-bicyclo[4.2.0]octene-carboxylate derivatives on the steel surface.

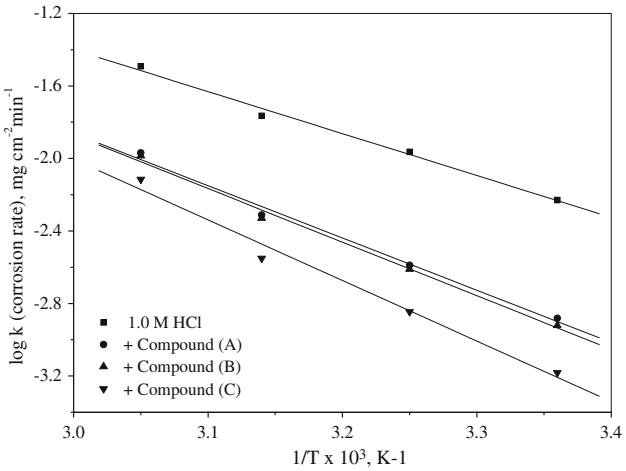

Fig. 5 Arrehenius plots (log K vs. $1/T$) for stainless steel type 304 in 1.0 M HCl in the absence and presence of 5×10^{-5} M of Compounds (A), (B), and (C)

3.2 Potentiodynamic polarization measurements

Potentiodynamic anodic and cathodic polarization scans were carried out at 25 °C in 1.0 M HCl with different concentrations of Compound (C) (Fig. 6). It can be seen from Fig. 6 that, in the presence of the inhibitor, the curves are shifted to lower current regions, showing the inhibition tendency of Compound (C). Similar curves were obtained for other compounds (not shown). This compound appeared to act as a mixed type inhibitor since both cathodic (hydrogen evolution) and anodic (metal dissolution) reactions were influenced by the presence of this compound in the corrosive medium, with the anodic effect being more significant. The cathodic curves showed parallel Tafel lines indicating that the hydrogen evolution reaction was enhanced. The values of various electrochemical parameters are summarized in Table 3.

The E_{corr} values were only slightly shifted to less negative values in the presence of the inhibitor indicating that these inhibitors act as anodic type inhibitors in 1.0 M HCl.

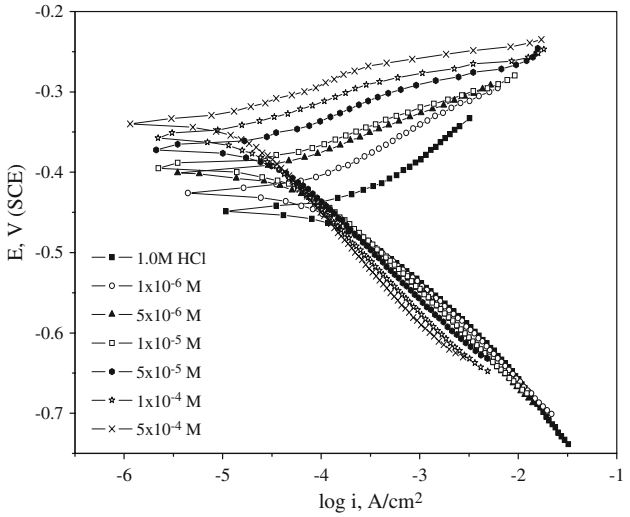

Fig. 6 Potentiodynamic polarization curves for the corrosion of stainless steel type 304 in 1.0 M HCl in the absence and presence of different concentrations of Compound (C) at 25 °C

Small changes in potentials can be a result of the competition of the anodic and the cathodic inhibiting reactions, and of the metal surface condition. From Table 3, the slopes of the cathodic Tafel lines (β_c) and anodic Tafel lines (β_a) are observed to change with addition of inhibitors, which indicates influence on both the cathodic and anodic reactions, the cathodic curves are more affected. Thus these inhibitors act as mixed type inhibitors for stainless steel in 1.0 M HCl.

The corrosion current densities were estimated by Tafel extrapolation of the cathodic and anodic curves to the open circuit corrosion potentials. Also, the results of this table show that an increase in inhibitor concentration is resulted in increased IE. It is evident from the results that the i_{corr} values decrease considerably in the presence of inhibitor. The polarization resistance (R_p) values of stainless steel type 304 in the absence and presence of different inhibitor concentrations are also given in Table 3. It is apparent that R_p increases with increasing inhibitor concentration. The IE% calculated from R_p values are also presented in Table 4. The degree of surface coverage; θ, at constant potential is given by the following relation [31, 32]:

$$\theta = \left[1 - \left(R_p/R_{(p\,inh)}\right)\right] \tag{12}$$

where R_p and $R_{(p\ inh)}$ are the polarization resistance of uninhibited and inhibited experiments, respectively. The percentage of inhibition efficiency, IE%, at each concentration was calculated using the equation:

$$IE\% = \left[1 - \left(R_p/R_{(p\,inh)}\right)\right] \times 100. \tag{13}$$

The IE% was found to increase with increasing the inhibitor concentration. The inhibition achieved by these compounds decreases in the following order: Compound (C) > Compound (B) > Compound (A). The inhibition efficiencies of investigated compounds obtained by

Table 3 Effect of concentrations of Compounds (A), (B), and (C) on the electrochemical parameters of stainless steel type 304 in 1.0 M HCl at 25 °C

Inhibitor	Conc. (M)	$-E_{OCP}$ (mV)	$-E_{corr}$ (mV)	i_{corr} (μA m^{-2})	$-\beta_c$ (mV dec^{-1})	β_a (mV dec^{-1})	R_p (Ω cm)	CR (mm year^{-1})
A	0.0	437.5	449	199.1	126.4	94.0	117.6	2.311
	1×10^{-6}	425.3	446	193.5	121.4	82.3	110.1	2.246
	5×10^{-6}	400.6	427	104.5	117.5	68.1	179.1	1.213
	1×10^{-5}	392.5	423	81.09	115.1	63.1	218.4	0.941
	5×10^{-5}	373.6	392	44.85	114.4	53.1	351.3	0.521
	1×10^{-4}	367.5	377	20.88	107.2	47.6	685.4	0.242
	5×10^{-4}	329.4	370	18.86	106.7	46.2	742.3	0.219
B	1×10^{-6}	423.9	436	115.9	117.7	76.7	174.0	1.345
	5×10^{-6}	384.5	427	96.57	116.3	75.9	206.5	1.121
	1×10^{-5}	388.6	414	51.38	110.0	62.5	336.8	0.596
	5×10^{-5}	330.8	392	25.44	102.0	52.7	593.5	0.295
	1×10^{-4}	362.6	371	22.99	114.5	50.3	660.0	0.267
	5×10^{-4}	356.2	364	19.27	113.6	46.8	747.5	0.224
C	1×10^{-6}	400.2	425	83.21	111.4	76.8	237.2	0.966
	5×10^{-6}	386.1	402	49.00	113.5	57.5	338.0	0.569
	1×10^{-5}	374.5	393	25.53	102.0	44.9	530.2	0.296
	5×10^{-5}	331.2	370	18.36	107.9	43.7	735.9	0.213
	1×10^{-4}	346.6	355	15.08	119.4	46.1	957.6	0.175
	5×10^{-4}	328.7	338	12.64	129.8	49.4	1230.0	0.147

Table 4 The inhibition efficiencies of different concentrations of Compounds (A), (B), and (C) for the corrosion of stainless steel type 304 in 1.0 M HCl at 25 °C as obtained from potentiodynamic polarization measurements

[Inhibitor] (M)	Compound (A)		Compound (B)		Compound (C)	
	IE (%), i_{corr}	IE (%), R_p	IE (%), i_{corr}	IE (%), R_p	IE (%), i_{corr}	IE (%), R_p
1×10^{-6}	2.8	6.8	41.8	32.4	58.2	50.4
5×10^{-6}	47.5	34.3	51.5	43.1	75.4	65.2
1×10^{-5}	59.3	46.2	74.2	65.1	87.2	77.8
5×10^{-5}	77.5	66.5	80.6	72.4	90.8	84.0
1×10^{-4}	89.5	82.8	88.5	82.2	92.4	87.7
5×10^{-4}	90.5	84.2	90.3	84.3	93.7	90.4

potentiodynamic polarization and by polarization resistance methods are in good agreement.

3.2.1 *Synergistic effect*

The increase in IE of organic compounds in the presence of some anions has been observed by several investigators [33–36] and was ascribed to synergistic effect. Trials to enhance the performance of the used inhibitors by addition of KI were carried out using potentiodynamic measurements. Figure 7 shows potentiodynamic polarization curves for stainless steel type 304 in 1.0 M HCl in the absence and presence of 1×10^{-6} M of Compound (C) without and with different concentrations (1×10^{-4}, 1×10^{-3}, 1×10^{-2} M) of KI at 25 °C. The obtained electrochemical values (E_{OCP}, E_{corr}, i_{corr}, β_c, β_a and R_p) are shown in Table 5. The calculated IE values are shown in Table 6. Results shown in the tables revealed that the presence of different concentrations of KI enhances the reduction of i_{corr} values for stainless steel in 1.0 M HCl, and the reduction in the rate increases with increasing the concentration of KI indicating that addition of KI increases the inhibiting action of the investigated inhibitors.

To further judge whether synergism is taking place, the synergism parameter; S_θ was calculated using the relation given by Aramiki and Hackerman and reported elsewhere [37].

$$S_\theta = 1 - \theta_{1+2}/1 - \theta'_{1+2} \quad (14)$$

where $\theta_{1+2} = (\theta_1 + \theta_2) - (\theta_1\theta_2)$; θ_1 is surface coverage by anion, θ_2 is surface coverage by cation and θ'_{1+2} is measured surface coverage by both anion and cation. The calculated synergism parameter; S_θ is given in Table 7. It is seen that all values of S_θ are less than unity which indicates the presence of antagonistic effects between the inhibitor and the iodide ion when adsorbed on the steel surface. Similar results obtained elsewhere [38, 39].

The order of increasing IE for the investigated inhibitors in the presence of 1×10^{-2} M KI and in case of constant concentration from the investigated inhibitors with different concentration of KI for stainless steel in 1.0 M HCl is as follows: Compound (C) > Compound (B) > Compound (A).

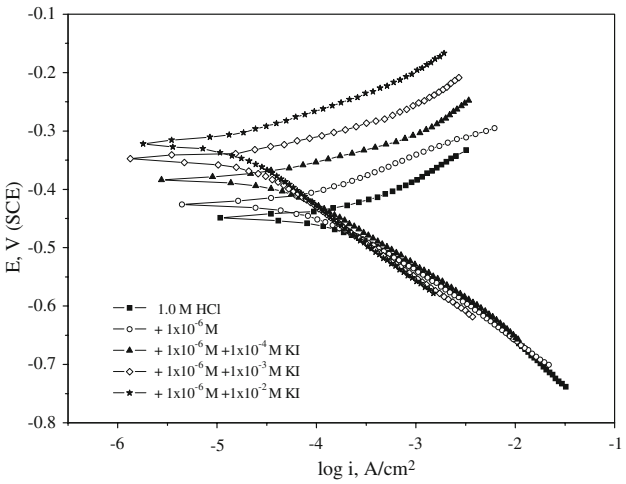

Fig. 7 Potentiodynamic polarization curves of stainless steel type 304 in 1.0 M HCl in the absence and presence of 1×10^{-6} M of Compound (C) and different concentrations of KI at 25 °C

3.3 Electrochemical impedance spectroscopy (EIS)

The corrosion of stainless steel type 304 in 1.0 M HCl in the presence of investigated compounds was investigated by EIS method at 25 °C after 20 min immersion. Nyquist and Bode plots in the absence and presence of investigated Compound (C) are presented in Figs. 8 and 9, respectively. Similar curves were obtained for other inhibitors. It is apparent that all Nyquist plots show a single capacitive loop, both in uninhibited and inhibited solutions. The impedance data of stainless steel in 1.0 M HCl are analyzed in terms of an equivalent circuit model (Fig. 10) which includes the solution resistance R_s or R_Ω and the double layer capacitance C_{dl} which is placed in parallel to the charge transfer resistance R_{ct} [40] due to the charge transfer reaction. For the Nyquist plots it's obvious that low frequency data are on the right side of the plot and higher

Table 5 Effect of addition of different concentrations of KI with 1×10^{-6} M of Compounds (A), (B), and (C) on the electrochemical parameters of stainless steel type 304 in 1.0 M HCl at 25 °C

Inhibitor	[KI] (M)	$-E_{OCP}$ (mV)	$-E_{corr}$ (mV)	i_{corr} (μA cm^{-2})	$-\beta_c$ (mV dec^{-1})	β_a (mV dec^{-1})	R_p (Ω cm)	CR (mm year^{-1})
A	–	425.3	446.3	193.5	121	82	110.1	2.246
	1×10^{-4}	347.3	380.9	77.66	119	90	288.7	0.902
	1×10^{-3}	307.6	345.2	23.61	116	77	853.7	0.274
	1×10^{-2}	243.9	316.9	17.12	128	82	1263.0	0.199
B	–	423.9	436.0	115.9	118	111	174.0	1.345
	1×10^{-4}	353.9	380.5	49.13	110	82	380.1	0.570
	1×10^{-3}	312.7	346.7	21.44	118	85	891.2	0.249
	1×10^{-2}	242.8	318.1	16.24	127	120	1309.0	0.188
C	–	400.2	424.8	83.21	111	77	237.2	0.966
	1×10^{-4}	357.8	382.8	43.68	111	62	395.3	0.507
	1×10^{-3}	317.3	348.2	17.50	115	55	924.4	0.203
	1×10^{-2}	276.2	322.3	14.63	128	67	1305.0	0.170

Table 6 Effect of addition of different concentrations of KI on the inhibition efficiency of 1×10^{-6}M of Compounds (A), (B), and (C) for the corrosion of stainless steel type 304 in 1.0 M HCl at 25 °C

[KI] (M)	Compound (A)		Compound (B)		Compound (C)	
	IE (%), i_{corr}	IE (%), R_p	IE (%), i_{corr}	IE (%), R_p	IE (%), i_{corr}	IE (%), R_p
–	2.8	−6.8	41.8	32.4	58.2	50.4
1×10^{-4}	61.0	59.3	75.3	69.1	78.1	70.3
1×10^{-3}	88.1	86.2	89.2	86.8	91.2	87.3
1×10^{-2}	91.4	90.7	91.8	91.0	92.7	91.0

Table 7 Synergism parameter (S_θ) for different concentrations of Compounds (A), (B), and (C) with 1×10^{-2} M KI for the corrosion of stainless steel type 304 in 1.0 M HCl at 25 °C

[Inhibitor] (M) + 1×10^{-2} M KI	Synergism parameter (S_θ), i_{corr}		
	Compound (A)	Compound (B)	Compound (C)
1×10^{-6}	1.029	0.646	0.521
5×10^{-6}	0.673	0.622	0.334
1×10^{-5}	0.561	0.367	0.224
5×10^{-5}	0.366	0.299	0.182
1×10^{-4}	0.203	0.201	0.150
5×10^{-4}	0.216	0.160	0.119

frequencies are on the left. This is true for EIS data where impedance usually falls as frequency rises (this is not true of all circuits). In the Bode plot, the impedance is plotted with log frequency on the *x*-axis and both the log of absolute value of the impedance and phase-shift on the *y*-axis. Unlike the Nyquist plot, the Bode plot explicitly shows frequency information. The phase angle does not reach 90° as it would for pure capacitive impedance. In the Bode plot at the highest frequencies, log R_s appears as a horizontal plateau while at the lowest frequencies, log($R_s + R_{ct}$) appears as a horizontal plateau.

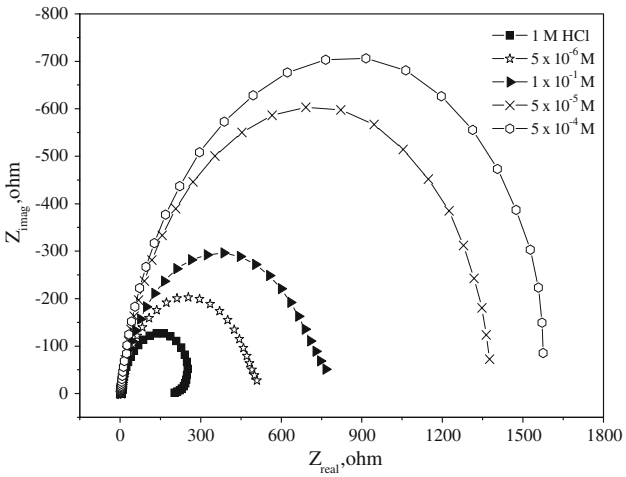

Fig. 8 The Nyquist plots for corrosion of stainless steel type 304 in 1.0 M HCl in the absence and presence of different concentrations of Compound (C) at 25 °C

The capacity of double layer (C_{dl}) can be calculated from the following equation

$$C_{dl} = \frac{1}{2\pi f_{max} R_{ct}} \tag{15}$$

where f_{max} is maximum frequency. The parameters obtained from impedance measurements are given in

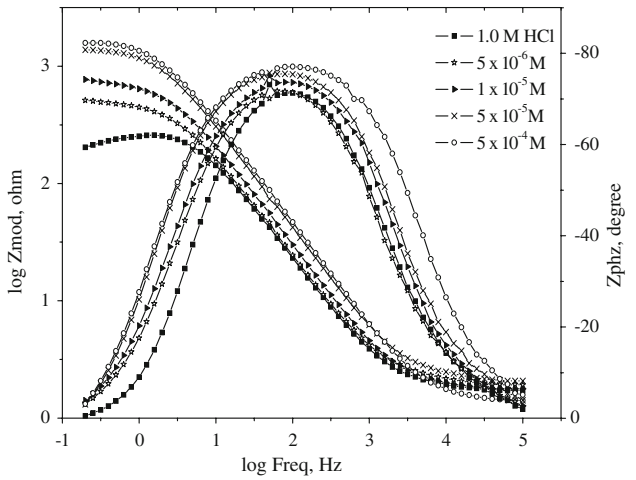

Fig. 9 The bode plots for corrosion of stainless steel type 304 in 1.0 M HCl in the absence and presence of different concentrations of Compound (C) at 25 °C

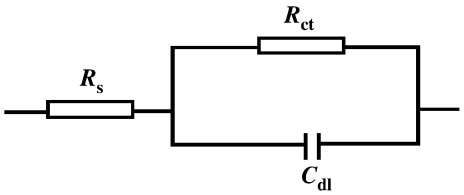

Fig. 10 The equivalent circuit model used to fit the experimental results

Table 8. It can see from Table 8 that the values of charge transfer resistance increase with inhibitor concentration [41] also, the IE% increases as the phase angle increases. In the case of impedance studies, IE% increases with inhibitor concentration in the presence of investigated inhibitors and the IE% of these investigated inhibitors is as follows: Compound (C) > Compound (B) > Compound (A). The impedance study confirms the inhibiting characters of these compounds obtained with weight loss and potentiodynamic polarization methods. It is also noted that the (C_{dl}) values tend to decrease when the concentration of these compounds increases. This decrease in (C_{dl}), which can result from a decrease in local dielectric constant and/or an increase in the thickness of the electrical double layer, suggests that these compounds molecules function by adsorption at the metal/solution interface [42].

The inhibiting effect of these compounds can be attributed to their parallel adsorption at the metal solution interface. The parallel adsorption is owing to the presence of one or more active center for adsorption. The chemisorption takes place by the formation of a chemical bond between the metal and the adsorbed molecule. Chemisorption involves charge or charge transfer from inhibitor molecule to the metal surface forming co-ordinate type bond [43].

Table 8 Electrochemical kinetic parameters obtained by EIS technique for the corrosion of stainless steel type 304 in 1.0 M HCl at different concentrations of Compounds (A), (B), and (C) at 25 °C

Inhibitor	Conc. (M)	C_{dl} (μF cm^{-2})	−Phase (degree)	R_p (Ω)	θ	IE (%)
A	0.0	71.35	71.3	234.6	–	–
	5×10^{-6}	73.07	72.0	333.5	0.297	29.7
	1×10^{-5}	71.04	71.4	349.8	0.329	32.9
	5×10^{-5}	55.18	73.3	683.1	0.657	65.7
	5×10^{-4}	44.68	75.0	991.5	0.763	76.3
B	5×10^{-6}	72.99	70.1	417.5	0.438	43.8
	1×10^{-5}	68.24	70.3	425.9	0.449	44.9
	5×10^{-5}	46.55	75.2	779.3	0.699	69.9
	5×10^{-4}	38.94	76.8	965.9	0.757	75.7
C	5×10^{-6}	72.06	71.6	430.6	0.455	45.5
	1×10^{-5}	58.12	73.5	628.0	0.626	62.6
	5×10^{-5}	41.81	75.2	1216.0	0.807	80.7
	5×10^{-4}	36.68	77.0	1404.0	0.833	83.3

3.4 Quantum chemical calculation

Quantum structure–activity relationships have been used to study the effect of molecular structure on IE of the investigated inhibitors. Table 9 shows the quantum chemical calculation parameters (E_{HUMO}, E_{LUMO}) and the energy band gap ($\Delta E = E_{HUMO} - E_{LUMO}$) is also listed. E_{HUMO} is often associated with the electron donating ability of the molecule. High E_{HUMO} values indicate that the molecule has a tendency to donate electrons to appropriate acceptor molecules with low energy empty molecular orbital. Increasing values of the E_{HUMO} facilitate adsorption (and therefore inhibition) by influencing the transport process through the adsorbed layer [44–46]. E_{LUMO} indicates the ability of the molecules to accept electrons. The lower values of the E_{LUMO}, the more probable it is that the molecule would accept electrons [44–46]. Low absolute values of the energy band gap (ΔE) gives good inhibition efficiencies, because the energy to remove an electron from the last occupied orbital will be low [47].

From this table it is evident that, the values of log i_{corr} are mostly depends upon the energies of the highest occupied molecular orbital (E_{HUMO}). It decreases with increasing E_{HUMO}. By other words, the IE values increase

Table 9 Quantum chemical parameters for 5×10^{-5} M of Compounds (A), (B), and (C) for corrosion of 304 SS in 1.0 M HCl

Compounds	−log $i_{corr.}$ (A cm^{-2})	$-E_{HOMO}$ (eV)	$-E_{LUMO}$ (eV)	$-\Delta E$ (eV)
(A)	4.3	7.95302	1.70113	6.25189
(B)	4.6	7.87107	1.679601	6.191469
(C)	4.7	7.61040	1.52402	6.08638

with decrease of ionization potential of the inhibitor molecule, which means that the inhibitor acts as an electron donor when blocking the corrosion reaction sites [48]. The results of these tables show that the energies of highest occupied molecular orbital (E_{HUMO}) decrease in the order: (C) > (B) > (A).

This is a good agreement with the previously mentioned experimental data obtained by weight loss and potentiodynamic polarization and EIS techniques.

3.5 Mechanism of inhibition

Many organic compounds with at least one polar unit containing atoms of nitrogen, sulfur oxygen are known to function as corrosion inhibitors. The polar unit is regarded as the reaction centre for the adsorption process. In such a case the adsorption bond strength is determined by the electron density on the atom acting as the reaction centre and by polarisability of the unit. Thus, polar organic compounds acting as corrosion inhibitors are adsorbed on the surface of the metal, forming a charge transfer complex between their polar atoms and the metal. The size, shape and orientation of the molecule and the electronic charge on the molecule determine the degree of adsorption and hence the effectiveness of the inhibitor.

The investigated inhibitors confer high protection to stainless steels corrosion in 1.0 M HCl and function through adsorption on the metal surface following Langmuir isotherm. The obtained results by weight loss, potentiodynamic polarization, and electrochemical impedance spectroscopy (EIS) techniques indicate that the extent of corrosion inhibition of the investigated compounds followed the following order: (C) > (B) > (A). It can be explained on the basis of adsorption. It is apparent from the molecular structure that these compounds can be adsorbed on the metal surface through the lone pair of electrons of oxygen and/or nitrogen and/or sulfur atoms and delocalized π-electrons of benzene ring. The difference in the inhibition efficiencies can be explained on the basis of the type and the number of hetero atoms in the cavity of these compounds. Also the IE values can be explained on the basis of the molecular weight; Compound (C) exhibits excellent IE due to its molecular weight (667.65) that may facilitate better surface coverage. Compound (B) comes after Compound (C) in IE because it has lesser molecular weight (546.58). Compound (A) has the lowest IE; this is because it has the lowest molecular weight (517.02) and has no aromatic ring.

4 Conclusions

3-Thiazinonyl-bicyclo [4.2.0] octene-carboxylate derivatives have proved to be good inhibitors for the corrosion of stainless steel type 304 in 1.0 M HCl solution. These inhibitors act as mixed type inhibitors but the anode is more polarized when an external current was applied and IE% was found to increase by increasing the inhibitor concentration and decrease with rising the temperature. The IE% obtained from electrochemical impedance spectroscopy and potentiodynamic polarization measurements show good agreement with those obtained from weight loss experiments.

The inhibition of stainless steel type 304 in 1.0 M HCl solution was found to obey Langmuir adsorption isotherm. The thermodynamic values obtained from this study indicate that the presence of the inhibitors increases the activation energy and the negative values of ΔG^{o}_{ads} indicate spontaneous adsorption of the inhibitors on the surface of the steel.

References

1. Szypowski AJ (2002) Br Corros J 37:141
2. Quraishi MA, Ansari FA, Jamal D (2003) Mater Chem Phys 77:687
3. Elachouri M, Hajji MS, Kertit S, Essassi EM, Salem M, Coudert R (1995) Corros Sci 37:381
4. Merari B, Elattar H, Traisnel M, Bentiss F, Larenee M (1998) Corros Sci 40:391
5. Bentiss F, Traisnel M, Lagrenee M (2000) Corros Sci 42:127
6. Elkadi L, Mernari B, Traisnel M, Bentiss F, Lagrenee M (2000) Corros Sci 42:703
7. Walker R (1975) Corros Sci 31:97
8. Bentiss F, Lagrenee M, Traisnel M, Lornez JC (1999) Corros Sci 41:789
9. Eddy NO (2008) PhD Thesis University of Calabar, Nigeria
10. Abdallah M (2004) Corros Sci 46(1):1981
11. Odoemelam SA, Ogoko EC, Ita BI, Eddy NO (2009) Port Electrochim Acta 27(1):57
12. Von Fraunhofer JA, Stidham SH (1991) J Biochem Eng 13(5):424
13. Solmaz R, Kardas G, Yazici B, Erbil M (2005) Prot Met 41(6):581
14. Abdallah M (2002) Corros Sci 44:717
15. El-Naggar MM (2007) Corros Sci 49(5):2236
16. Arslan T, Kandemirli F, Ebenso EE, Love I, Alemu H (2009) Corros Sci 51:35
17. Ashassi-Sorkhabi H, Shabani B, Aligholipour B, Seifzadeh D (2006) Appl Surf Sci 252:4039
18. Ehteshamzada M, Shahrabi T, Hosseini MG (2006) Appl Surf Sci 252:2949
19. Dadgarnezhad A, Sheikhshoaie I, Baghaei F (2004) Asian J Chem 16:1109
20. Shokry H, Yuasa M, Sekine I, Issa RM, El-Baradie HY, Gomma GK (1998) Corros Sci 40:2173
21. El-Kanouni A, Kertti S, Srhiri A, Bachir K (1996) Bull Electrochem 12:517
22. Talati JD, Modi RM (1986) Trans SEAST 11: 259
23. Szklarska-Smiaiowska Z (1991) Electrochemical and optical techniques for the study of metallic corrosion. Kluwer Academic, The Netherlands, p 545
24. Langmuir I (1947) J Amer Chem Soc 39:1848

25. Khamis E (1990) Corrosion 46:476
26. El-Awady YA, Ahmed AI (1985) J Ind Chem 24A:601
27. Putilova IK, Balezin S, Barannik V (1960) Metallic corrosion inhibitors. Pergamon, Oxford, p 30
28. Zhao TP, Mu GN (1999) Corros Sci 41:1937
29. Fouda AS, Mostafa HA, El-Taib F, El-Ewady GY (2005) Corros Sci 47:1988
30. Fouda AS, Al-Sawary AA, Ahmed FSh, El-Abbasy HM (2009) Corros Sci 51:485
31. Ammar IA, Darwish S (1967) Corros Sci 7:679
32. Fisher H (1960) Ann Univ Ferrera Sez 3(Suppl 3):1
33. Umoren SA, Ogbobe O, Ebenso EE (2006) Trans SAEST 41:74
34. Umoren SA, Ebenso EE (2007) Mater Chem Phys 106:387
35. Oguzie EE, Ebenso EE (2006) Pigment Resin Technol 35:30
36. Gomma GK (1998) Mater Chem Phys 55:241
37. Aramaki K, Hackerman N (1969) J Electrochem Soc 116:568
38. El-Gaber AS, Fouda AS, El-Desoky AM (2008) Sci Technol Mater 20(3):71
39. Li X, Deng S, Fu H, Mu G (2008) Corros Sci 50:2635
40. Sekine I, Sabongi M, Hagiuda H, Oshibe T, Yuasa M, Imahc T, Shibata Y, Wake T (1992) J Electrochem Soc 139:3167
41. Larabi L, Benali O, Mekelleche SM, Harek Y (2006) J Appl Surf Sci 253:1371
42. Lagrenee M, Mernari B, Bouanis B, Traisnel M, Bentiss F (2002) Corros Sci 44:573
43. Khamis E, Bellucci F, Latahision RM, El-Ashry ESh (1991) Corrosion 47(9):667
44. Wanklyn JN (1981) Corros Sci 21:211
45. Tullmin MAA, Robinson FPA (1988) Corrosion 44:664
46. Ciesak WR, Duquette DJ (1985) J Electrochem Soc 132:533
47. Galvole JR, Lumsden JB, Stechle RW (1978) J Electrochem Soc 125:1204
48. Sugimoto K, Sawada Y (1976) Corrosion 32:347